Non-local optics of the near field lens

2005 J. Phys.: Condens. Matter 17 1803

(http://iopscience.iop.org/0953-8984/17/12/004)

INSTITUTE OF PHYSICS PUBLISHING JOURNAL OF PHYSICS: CONDENSED MATTER

J. Phys.: Condens. Matter **17** (2005) 1803–1810 doi:10.1088/0953-8984/17/12/004

Non-local optics of the near field lens

R Ruppin[1]

The Blackett Laboratory, Imperial College, London SW7 2AZ, UK

Received 27 October 2004, in final form 17 February 2005
Published 11 March 2005
Online at stacks.iop.org/JPhysCM/17/1803

Abstract

The effects of non-locality on the focusing properties of a thin metal slab, with the real part of the permittivity equal to -1, are evaluated. Non-local effects are introduced by employing the wavenumber-dependent plasmon energy of the hydrodynamic model. Non-locality affects the dispersion of the surface plasmons, the transmissivity of the slab, and hence also its imaging ability. The results of numerical calculations for silver slabs are presented.

1. Introduction

It has been predicted by Veselago [1] that a slab with permittivity and permeability given by $\varepsilon = -1$ and $\mu = -1$, respectively, would act as a lens. Pendry [2] has shown that the resolution of such a lens is not limited by the classical diffraction limit. This remarkable property of the negative index material lens is due to its ability to amplify the evanescent near-field components of the source, which describe the finest details of the object. Furthermore, for thin enough films, for which the electrostatic approximation applies, near-field focusing of p polarized fields might be achieved even when only the condition $\varepsilon = -1$ is satisfied [2]. For this purpose silver seems to be the most promising material in the optical range. Following this idea, a number of investigations of the imaging properties of negative permittivity slabs in general [3–5], and of thin silver films in particular [2, 6–9], have been performed, and potential applications to sub-wavelength optical lithography have been suggested [10, 11].

The ability of the lens to amplify evanescent waves is related to the presence of surface plasmon modes [2]. In all theoretical discussions of these effects, the surface modes were assumed to be dispersionless in the large k limit, where k is the wavevector component parallel to the surface. However, due to non-local effects (also called spatial dispersion effects) there occurs a k dependence of the modes at large k. A simple way of including these non-local effects is to employ the hydrodynamic model, as will be done in the calculations presented here. In this model the dispersion of the bulk plasmons is given by [12]

$$\omega^2(q) = \omega_p^2 + \beta^2 q^2 \tag{1}$$

where ω_p is the plasma frequency, q is the wavenumber and $\beta^2 = \frac{3}{5}v_F^2$, where v_F is the Fermi velocity. The application of the hydrodynamic model to the calculation of optical properties

[1] On leave from: Soreq NRC, Yavne 81800, Israel.

and surface plasmon dispersion has been reviewed in [13, 14]. The Fresnel equations for the reflection and transmission of an incident electromagnetic plane wave, which were developed for a local medium, have to be modified when dealing with a non-local medium, so as to allow for the direct optical excitation of longitudinal plasmon modes, as pointed out by Sauter [15]. Melnyk and Harrison [16] have calculated the optical properties of a non-local metal. They have found that for a semi-infinite medium the influence of non-locality on the reflectivity is hardly discernible. However, for films with thickness of the order of $d = 10$ nm or less, the absorption, reflection and transmission spectra differ perceptibly from those derived from the local theory. The main effect arising from non-locality was the excitation of standing bulk plasma waves inside the thin films. These manifest themselves in the optical spectra as a series of subsidiary peaks in the frequency region $\omega > \omega_p$. These predictions were confirmed experimentally in optical experiments in which thin potassium [17] and silver [18, 19] films have been used. In imaging applications of Ag films, the typical thickness is of the order of $d = 40$ nm. This value of d is large enough so that the effects of non-locality on direct optical properties, such as reflection or transmission spectra, would be negligible. However, as will be shown in section 2, the slab surface plasmons of the non-local model are dispersive at large wavevectors. These large wavevector modes are involved in the amplification of the evanescent components of the source field. Thus their dispersion may influence the imaging capability of the thin film lens, and in section 3 we investigate this effect in detail.

2. Surface polaritons of non-local material

2.1. Semi-infinite medium

We assume that the non-local material occupies the $z > 0$ half-space, and that the medium at $z < 0$ has a frequency-independent dielectric constant ε_1. For the case of p polarization, and assuming a $e^{-i\omega t}$ time dependence, the fields in the region $z < 0$ can be written in the form

$$\vec{H}^{(1)} = \hat{a}_y A e^{\alpha z} e^{ikx} \tag{2}$$

$$\vec{E}^{(1)} = -\frac{c}{\omega\varepsilon_1} A(i\alpha\hat{a}_x + k\hat{a}_z) e^{\alpha z} e^{ikx} \tag{3}$$

where $\hat{a}_x, \hat{a}_y, \hat{a}_z$ are unit vectors in the x, y and z directions, respectively, and

$$\alpha = \left(k^2 - \varepsilon_1 \frac{\omega^2}{c^2}\right)^{1/2}. \tag{4}$$

The transverse fields in the region $z > 0$ are given by

$$\vec{H}_T^{(2)} = \hat{a}_y B e^{-\delta z} e^{ikx} \tag{5}$$

$$\vec{E}_T^{(2)} = \frac{c}{\omega\varepsilon(\omega)} B(i\delta\hat{a}_x - k\hat{a}_z) e^{-\delta z} e^{ikx} \tag{6}$$

where

$$\delta = \left(k^2 - \varepsilon(\omega)\frac{\omega^2}{c^2}\right)^{1/2} \tag{7}$$

and $\varepsilon(\omega)$ is the transverse dielectric function of the metal, for which the local approximation can be used, as discussed by Fuchs and Kliewer [20].

For the longitudinal fields in the region $z > 0$ we use the form

$$\vec{E}_L^{(2)} = D\left(\hat{a}_x + i\frac{\gamma}{k}\hat{a}_z\right) e^{-\gamma z} e^{ikx} \tag{8}$$

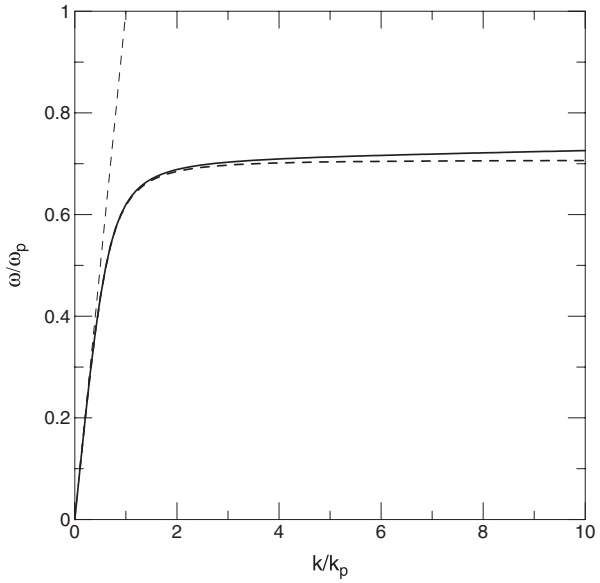

Figure 1. Dispersion curve of a surface plasmon–polariton at the interface between a semi-infinite metallic medium and vacuum. Full curve: non-local calculation; broken curve: local approximation.

where, for the hydrodynamic model,

$$\gamma = [k^2 + (\omega_p^2 - \omega^2)/\beta^2]^{1/2}. \tag{9}$$

Since we are allowing for the existence of longitudinal modes, the usual boundary conditions of the continuity of the tangential components of the fields at $z = 0$ have to be augmented by an additional boundary condition. Melnyk and Harrison [16] have shown that the appropriate boundary condition is the continuity of the normal component of the displacement current, which implies the continuity of E_z. The three boundary conditions yield a system of three linear homogeneous equations for the coefficients A, B and D. Equating to zero the determinant of this system yields the surface polariton dispersion relation:

$$k^2[\varepsilon_1 - \varepsilon(\omega)] = \gamma[\alpha\varepsilon(\omega) + \delta\varepsilon_1]. \tag{10}$$

For $\varepsilon_1 = 1$ this is equivalent to the result derived by Sturm [21]. The dispersion relation (10) is shown by the full curve of figure 1. For this calculation the form

$$\varepsilon(\omega) = 1 - \frac{\omega_p^2}{\omega^2} \tag{11}$$

was used and the value $\varepsilon_1 = 1$ was employed. The parallel component of the wavenumber is given in units of $k_p = \omega_p/c$ and the frequency in units of ω_p. In this dimensionless representation, the only parameter of the non-local medium which has to be specified is the ratio v_F/c, for which the typical value of $1/200$ was employed. The standard dispersion relation, obtained from local theory, is

$$\alpha\varepsilon(\omega) + \beta\varepsilon_1 = 0 \tag{12}$$

and this is shown by the broken curve of figure 1. It can be seen that for large k the broken curve approaches the frequency ω_S, defined by $\varepsilon(\omega_S) = -\varepsilon_1$, which yields the value $\omega_S = \omega_p/\sqrt{2}$. The non-local dispersion curve increases linearly at large k. The rate of this increase can be

evaluated by taking the non-retarded limit of equation (10) and expanding to first order in k, yielding

$$\frac{\omega}{\omega_{\rm p}} = \frac{1}{\sqrt{2}}\left[1 + \left(\frac{3}{10}\right)^{1/2} \frac{v_{\rm F}k}{\omega_{\rm p}}\right] \tag{13}$$

which is the known electrostatic surface plasmon dispersion relation of the hydrodynamic model [20, 22].

2.2. Slab

We assume that the non-local material occupies the region $0 < z < d$, and that the medium outside the slab has a frequency-independent dielectric constant ε_1. For the case of p polarization, the fields in the region $z < 0$ can be written in the form

$$\vec{H}^{(1)} = \hat{a}_y A {\rm e}^{\alpha z}{\rm e}^{{\rm i}kx} \tag{14}$$

$$\vec{E}^{(1)} = -\frac{c}{\omega\varepsilon_1} A({\rm i}\alpha\hat{a}_x + k\hat{a}_z){\rm e}^{\alpha z}{\rm e}^{{\rm i}kx}. \tag{15}$$

The transverse fields inside the slab are given by

$$\vec{H}^{(2)} = \hat{a}_y(B{\rm e}^{\delta z} + D{\rm e}^{-\delta z}){\rm e}^{{\rm i}kx} \tag{16}$$

$$\vec{E}^{(2)}_{\rm T} = \frac{c}{\omega\varepsilon(\omega)}[-B({\rm i}\delta\hat{a}_x + k\hat{a}_z){\rm e}^{\delta z} + D({\rm i}\delta\hat{a}_x - k\hat{a}_z){\rm e}^{-\delta z}]{\rm e}^{{\rm i}kx} \tag{17}$$

and the longitudinal field is

$$\hat{E}^{(2)}_{\rm L} = \left[F\left(\hat{a}_x - {\rm i}\frac{\gamma}{k}\hat{a}_z\right){\rm e}^{\gamma z} + G\left(\hat{a}_x + {\rm i}\frac{\gamma}{k}\hat{a}_z\right){\rm e}^{-\gamma z}\right]{\rm e}^{{\rm i}kx}. \tag{18}$$

The fields in the region $z > 0$ are written in the form

$$\vec{H}^{(3)} = \hat{a}_y K {\rm e}^{-\alpha z}{\rm e}^{{\rm i}kx} \tag{19}$$

$$\vec{E}^{(3)} = \frac{c}{\omega\varepsilon_1} K({\rm i}\alpha\hat{a}_x - k\hat{a}_z){\rm e}^{-\alpha z}{\rm e}^{{\rm i}kx}. \tag{20}$$

Applying the boundary conditions of the continuity of H_y, E_x and E_z at $z = 0$ and d yields a system of six homogeneous linear equations for the six coefficients A, B, D, F, G, K. The resulting dispersion relation is

$$\begin{vmatrix} 1 & -1 & -1 & 0 & 0 & 0 \\ -\frac{\alpha c}{\omega\varepsilon_1} & \frac{\delta c}{\omega\varepsilon(\omega)} & -\frac{\delta c}{\omega\varepsilon(\omega)} & 1 & 1 & 0 \\ \frac{kc}{\omega\varepsilon_1} & -\frac{kc}{\omega\varepsilon(\omega)} & -\frac{kc}{\omega\varepsilon(\omega)} & -\frac{\gamma}{k} & \frac{\gamma}{k} & 0 \\ 0 & {\rm e}^{\delta d} & {\rm e}^{-\delta d} & 0 & 0 & -1 \\ 0 & \frac{\delta c}{\omega\varepsilon(\omega)}{\rm e}^{\delta d} & -\frac{\delta c}{\omega\varepsilon(\omega)}{\rm e}^{-\delta d} & {\rm e}^{\gamma d} & {\rm e}^{-\gamma d} & \frac{\alpha c}{\omega\varepsilon_1} \\ 0 & \frac{kc}{\omega\varepsilon(\omega)}{\rm e}^{\delta d} & \frac{kc}{\omega\varepsilon(\omega)}{\rm e}^{-\delta d} & \frac{\gamma}{k}{\rm e}^{\gamma d} & -\frac{\gamma}{k}{\rm e}^{-\gamma d} & -\frac{kc}{\omega\varepsilon_1} \end{vmatrix} = 0. \tag{21}$$

As in the local case, there exist two surface polariton branches, resulting from the interaction of the surface modes localized near the two surfaces of the slab. The dispersion curves of the surface plasmon–polaritons, as calculated from (21), are shown in figure 2. The slab thickness d is given by $k_{\rm p}d = 0.5$, and again we assume that $v_{\rm F}/c = 1/200$. The dispersion curves obtained from the local theory are also shown. These were calculated from the equations

$$\varepsilon(\omega) = -\frac{\delta}{\alpha}\tanh(\delta d/2) \tag{22}$$

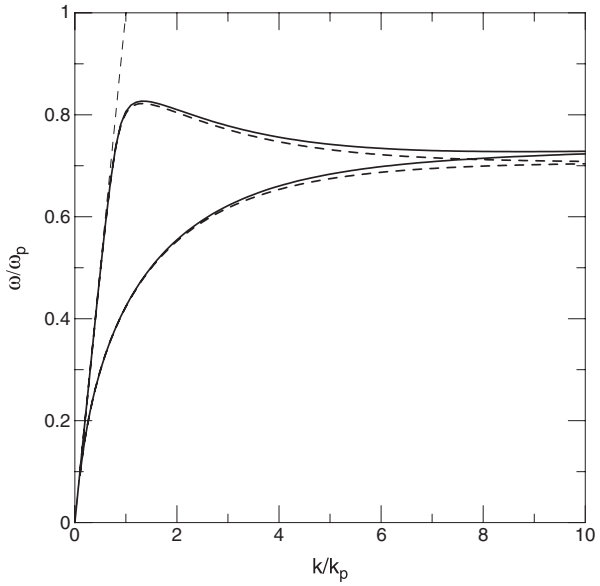

Figure 2. Dispersion curves of surface plasmon–polaritons of a metal slab of thickness $k_p d = 0.5$ in vacuum. Full curve: non-local calculation; broken curve: local approximation.

and

$$\varepsilon(\omega) = -\frac{\delta}{\alpha}\coth(\delta d/2) \tag{23}$$

for the high and low branch, respectively [23]. While for small k the local and non-local modes overlap, as k increases the non-local curves are always higher than the corresponding local ones. In the large k limit the broken curves approach the limiting value of $\omega/\omega_p = 1/\sqrt{2}$, while the full curves increase linearly with k, according to the rule (13).

3. Near field imaging

We now calculate the focusing properties of a thin silver slab. For a slab of thickness d the object plane and the image plane are located at distances of $d/2$ from the two surfaces of the slab. Thus, for the geometry of section 2.2 the object plane is at $z = -d/2$, and the image plane is at $z = 3d/2$. The source fields are expanded in a Fourier integral. Restricting the field variation to one transverse direction (no y dependence) this expansion has the form

$$\vec{E}(k) = \frac{1}{\sqrt{2\pi}}\int_{-\infty}^{\infty}\vec{E}\left(x, z = -\frac{d}{2}\right)\mathrm{e}^{-\mathrm{i}kx}\,\mathrm{d}x. \tag{24}$$

Here, as in section 2, k denotes the x component of the wavevector. The z dependence of the fields is given by $\exp(\mathrm{i}k_z z)$, where $k_z^2 = \varepsilon_1(\omega/c)^2 - k^2$. The field emanating from the source will include both propagating modes, with real k_z, and evanescent modes, with imaginary k_z. The latter occur when $k^2 > \varepsilon_1(\omega/c)^2$, i.e., for the higher Fourier components, which describe the finer details of the object. For each Fourier component the field at the image plane is calculated, and the image is obtained by the inverse transform

$$\vec{E}\left(x, z = \frac{3d}{2}\right) = \frac{1}{\sqrt{2\pi}}\int_{-\infty}^{\infty}\vec{E}(k)T(k)\mathrm{e}^{2\mathrm{i}k_z d}\mathrm{e}^{\mathrm{i}kx}\,\mathrm{d}k \tag{25}$$

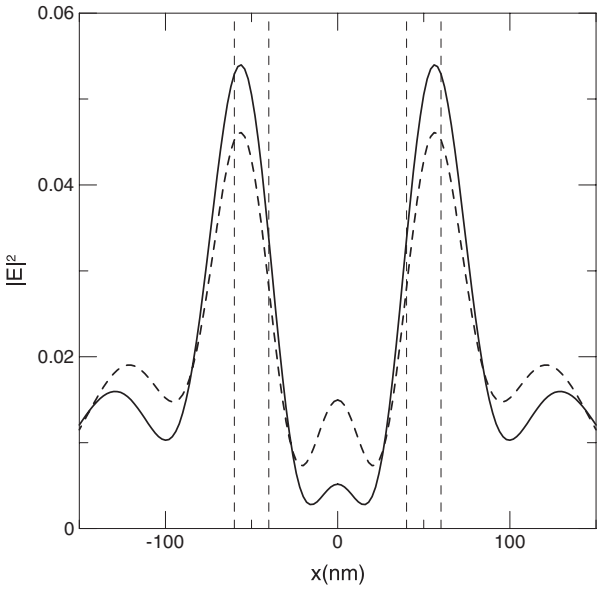

Figure 3. Field intensity at the image plane for a silver film of thickness $d = 40$ nm. Full curve: non-local calculation; broken curve: local approximation. The vertical broken lines show the position of the object.

where $T(k)$ is the transmission coefficient of the slab. For the local case the classical formulae for the transmission [2] are employed. For the non-local case the method of calculation is similar to that presented in section 2, except that now an incident field has to be added. Explicit formulae for the transmission coefficient for this case have been presented by Melnyk and Harrison [16]. For the object field we assume a double spike structure of unity amplitude. The two spikes have a width of 20 nm and are separated by a distance of 100 nm. The calculations are performed for $\hbar\omega = 3.68$ eV. Now we do not use the free electron like form (11) of the dielectric constant, but employ the experimentally measured value of the dielectric constant of silver at this frequency, $\varepsilon = -1 + 0.3\mathrm{i}$ [24]. We also add a damping term to the longitudinal modes, using the experimental value of the damping frequency [18]. The results for a slab of thickness 40 nm are shown in figure 3. The image obtained from the full non-local calculation is somewhat better than that derived from the local theory: the images of the spikes are slightly higher, while the unwanted side lobes are reduced in amplitude. The difference between the two approaches becomes even more perceptible for $d = 50$ nm, as shown in figure 4. At this thickness the image derived from the local theory has deteriorated due to retardation effects, while the one obtained from the non-local calculation is still useful.

4. Discussion

We have investigated the influence of non-locality on the near field lens made of a metallic slab having a negative permittivity. The non-local properties of the slab material were characterized by the hydrodynamic model. Using this model, we have calculated the surface plasmon dispersion curves and found that for large wavevectors they deviate from the corresponding curves of the local model. Whereas in the local case the curves become dispersionless at large wavevectors, in the non-local case the frequency increases linearly with the wavevector. The effect of this dispersion on the imaging properties of a silver slab has been evaluated.

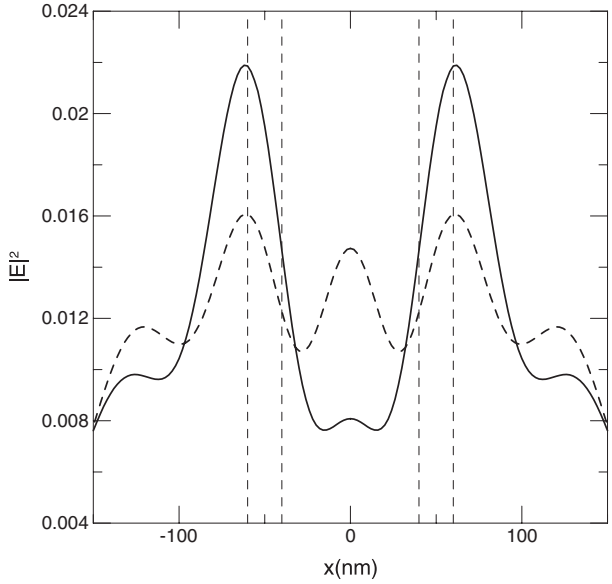

Figure 4. Field intensity at the image plane for a silver film of thickness $d = 50$ nm. Full curve: non-local calculation; broken curve: local approximation. The vertical broken lines show the position of the object.

For a silver slab thickness of the order of 40 nm, which is the size typically considered for applications [10], the image quality is slightly better when non-local effects are taken into account. This we attribute to the slight upward shift of the lower surface plasmon branch (see figure 2), which brings it into better overlap with the $\varepsilon(\omega) = -1$ line in the k range of interest.

In the treatment presented here the changes in the electron density near the slab surfaces have been neglected. The implicit assumption is that the electron density changes abruptly from its bulk value to zero. The effects of a non-abruptly decreasing electron density can be incorporated into the hydrodynamic model by assuming that in a thin surface layer the electron density differs from its bulk value [25, 26]. A more accurate description of both the ground state electronic properties in the surface region and the non-local response of surface electrons to incident electromagnetic fields is provided by the density functional method [27]. Whatever method is used, when a non-abrupt electron density profile is incorporated, it is usually found that the surface plasmon frequency shifts downwards for small k, and only after reaching a minimum it begins to rise. This type of dispersion was also observed experimentally on, for example, K, Na, Cs, Al, Mg [27]. Future refinements of the present approach should take the non-abrupt density profile into account. For silver, further complications, due to s–d hybridization, occur. When these were incorporated into the density functional calculations [28, 29], it was found that the dispersion of the surface plasmon of Ag is positive, even at small wavevectors, as also observed experimentally [30]. Thus, the trend of the silver surface plasmon dispersion agrees fortuitously with that obtained from the model employed here. This implies that the modifications which will result form inclusion of a non-abrupt density profile will be relatively small for silver.

Acknowledgment

I thank the EC under project FP6-NMP4-CT-2003-505699 for financial support.

References

[1] Veselago V G 1968 *Sov. Phys.—Usp.* **10** 509
[2] Pendry J B 2000 *Phys. Rev. Lett.* **85** 3966
[3] Shamonina E, Kalinin V A, Ringhofer K H and Solymar L 2001 *Electron. Lett.* **37** 1243
[4] Shen J T and Platzman P M 2002 *Appl. Phys. Lett.* **80** 3286
[5] Lu W T and Sridhar S 2003 *Microw. Opt. Technol. Lett.* **39** 282
[6] Ramakrishna S A, Pendry J B, Schurig D, Smith D R and Schultz S 2002 *J. Mod. Opt.* **49** 1747
[7] Fang N, Liu Z, Yen T J and Zhang X 2002 *Opt. Express* **11** 682
[8] Liu Z, Fang N, Yen T J and Zhang X 2003 *Appl. Phys. Lett.* **83** 5184
[9] Kik P G, Maier S A and Atwater A 2004 *Phys. Rev.* B **69** 045418
[10] Blaikie R J and McNab S J 2002 *Microelectron. Eng.* **61** 97
[11] Melville D O S, Blaikie R J and Wolf C R 2004 *Appl. Phys. Lett.* **84** 4403
[12] Jackson J D 1975 *Classical Electrodynamics* (New York: Wiley)
[13] Boardman A D 1982 *Electromagnetic Surface Modes* ed A D Boardman (New York: Wiley) p 1
[14] Forstmann F and Gerhardts R R 1986 *Metal Optics Near the Plasma Frequency* (Berlin: Springer)
[15] Sauter F 1967 *Z. Phys.* **203** 488
[16] Melnyk A R and Harrison M J 1970 *Phys. Rev.* B **2** 835
[17] Anderegg M, Feuerbacher B and Fitton B 1971 *Phys. Rev. Lett.* **27** 1565
[18] Lindau I and Nilsson P O 1971 *Phys. Scr.* **3** 87
[19] Abeles F, Borensztein Y, de Crescenzi M and Lopez-Rios T 1980 *Surf. Sci.* **101** 123
[20] Fuchs R and Kliewer K L 1971 *Phys. Rev.* B **3** 2270
[21] Sturm K 1968 *Z. Phys.* **209** 329
[22] Ritchie R H 1963 *Prog. Theor. Phys. (Kyoto)* **29** 607
[23] Kliewer K L and Fuchs R 1966 *Phys. Rev.* **144** 495
[24] Johnson P B and Christy R W 1972 *Phys. Rev.* B **6** 4370
[25] Bennett A J 1970 *Phys. Rev.* B **1** 203
[26] Boardman A D, Paranjape B V and Teshima R 1975 *Surface Sci.* **49** 275
[27] Liebsch A 1997 *Electronic Excitations at Metal Surfaces* (New York: Plenum)
[28] Liebsch A 1993 *Phys. Rev. Lett.* **71** 145
[29] Liebsch A and Schaich W L 1995 *Phys. Rev.* B **52** 14219
[30] Suto S, Tsuei K D, Plummer E W and Burstein E 1989 *Phys. Rev. Lett.* **63** 2590